Available online at www.sciencedirect.com
ScienceDirect
Pattern Recognition 41 (2008) 77–89
PATTERN RECOGNITION
THE JOURNAL OF THE PATTERN RECOGNITION SOCIETY
www.elsevier.com/locate/pr

Chromosome classification based on the band profile similarity along approximate medial axis☆

Jau-hong Kao, Jen-hui Chuang*, Tsaipei Wang

Department of Computer Science, National Chiao Tung University, 1001 Ta Hsueh Road, Hsinchu, Taiwan

Received 7 July 2006; received in revised form 18 May 2007; accepted 21 May 2007

Abstract

Automated chromosome classification is an essential task in cytogenetics and has been an important pattern recognition problem. Numerous attempts were made in the past to characterize chromosomes for the purposes of clinical and cancer cytogenetics research. It is important to determine good features and develop feature extraction schemes for chromosome classification. In this paper we propose efficient approaches for medial axis determination and profile matching of human chromosomes without identifying centromeres. The medial axis determination is based on simple cross-section analysis. The features of the band profile obtained along the axis are then used to classify a chromosome based on a subsequence matching technique. Using a special indexing structure, we are able to perform fast similarity search and dynamic insertion and deletion over the established subsequence database of chromosome profiles. According to the experimental results, the developed adaptive system can automatically and efficiently determine the medial axis of a given chromosomes, and achieve satisfactory classification results.

Keywords: Chromosome classification; Medial axis; Sequence similarity; Sequence matching

1. Introduction

Chromosome classification is an essential task in cytogenetics and has been an important pattern recognition problem. Numerous attempts were made in the past to characterize chromosome for prenatal screening, genetic syndrome diagnosis, cancer pathology research, and environmentally induced mutagen dosimetry. However, chromosome classification and analysis, which create karyotypes, are manually performed in most cytogenetics laboratories nowadays in a repetitive, time-consuming and therefore expensive procedure [1,2]. Hence, the development of computerized methods to automate the procedure has attracted much attention. Such a system should be able to extract chromosome image features and use these features for classifier training as well as actual classification tasks. It is important to determine optimum features and develop a feature description scheme for chromosome classification. In general, the features used for chromosome classification include shape descriptors, such as length and centromere index, and band pattern representation. Lengths are simple to measure if the chromosomes are segmented properly, but the centromeres are subtle and sometimes difficult to locate. Several shape-based techniques have been proposed. In Ref. [3], the curvature of each chromosome is studied, and the feature vector extracted from the curvature is used for the classification of each chromosome. The wavelet packet transform and Fourier transform for shape representation also motivate the development of the approaches for chromosome classification in Ref. [4]. The performance of shape-based approaches depends heavily on the quality of the input images as well as the resolution of the boundary of the segmented chromosome. Since length and centromere index by themselves cannot be used to classify human chromosomes reliably into their 24 classes, band patterns produced by modern specimen staining techniques have been used as an important feature for both manual and automated chromosome classification.

☆ This work is partly supported by Lumens Digital Optics, Inc., and by Ministry of Economic Affairs, Taiwan, under Grant no. 95-EC-17-A-02-S1-032.

* Corresponding author. Tel.: +886 3 5712121x31979.
E-mail addresses: gis88804@cis.nctu.edu.tw (J.-h. Kao), jchuang@cs.nctu.edu.tw (J.-h. Chuang), wangts@cs.nctu.edu.tw (T. Wang).

0031-3203/$30.00
doi:10.1016/j.patcog.2007.05.016

While band patterns are often used in the discrimination of human chromosomes into their corresponding ISCN categories [5], they are difficult to extract automatically in general. For example, chromosomes are often bent, and the colors of the pixels within the same band produced by the staining process are usually nonuniform. As a result, the sampled gray-values are often noisy and contain outliers [6,7]. As stated in Refs. [1,8], the combination of features from both band pattern and shape representation is able to reduce the error rate of karyotyping systems.

A medial axis transform is usually performed as a basis for measuring a band profile, and therefore is a required and particularly critical step. The authors of Ref. [9] obtain the band profile by integrating the intensities along cross-sections perpendicular to the medial axis, or longitudinal axis, but severely bent chromosomes could be difficult to straighten. In general, medial axis determination usually involves (i) an iterative thinning process, and (ii) a pruning process to eliminate spurious branches produced by (i), and is a difficult task [10]. Many approaches have been proposed to perform this task [6,10–12]. In Refs. [10,12], the authors obtain the medial axis based on the dominant points of the contour and cubic splines of the boundary, and use a simple constrained classifier to classify chromosomes. Some medial axis calculation methods are based on second order moments of the chromosome gray-values, but they are not applicable to bent chromosomes [11].

To represent extracted chromosome band patterns, several transforms have been proposed. Some of them are based on discrete Fourier transform (DFT) to derive global descriptors of the density profile [13]. The weighted density distribution (WDD)-based approach correlates the band profile with a set of basis functions, and the correlations, rather than the profile itself, serve as the representation of the chromosome [14,15]. Markov chain-based methods quantize the band profiles of chromosomes and represent them as chains of symbols [16]. Neural network (NN)-based approaches are proposed to classify chromosomes as well [1,9,17,18]. In Ref. [1], a multi-layer perceptron is implemented which uses chromosome length, centromere index, and 15 points from a 64-element density profile as features. The classifiers are highly dependent on the representation of chromosome features.

In this paper, we propose a novel approach for chromosome classification based on band profile similarity. The band profiles extracted along approximate medial axes are partitioned into subsequences, and the classification is achieved by performing subsequence matching over a dynamically updated database. In our experiments, the chromosome images have been segmented by Lumens Digital Optics Inc., Taiwan. Because the centromere positions, which are often important features [6,15,19–21], are difficult to identify in these images, the proposed approach uses only band profiles for classification. Since chromosomes have no branches and their shapes are elongated with nearly uniform width, our method approximates the medial axis by simple cross-section analysis along four scan-line directions as described in Section 2. To improve the robustness of band profile extraction, gray-values at three different locations on each cross-section along the medial axis are sampled and combined, as discussed in Section 3. Section 4 describes the classification approach based on subsequence matching. Section 5 presents the experimental results and Section 6 gives the conclusion of this paper.

2. Medial axis extraction

The fact that chromosomes can be very sinuous, especially for the classes of longer ones, results in major challenges for automatic classification of a chromosome, or the composition of a karyotype. Fig. 1 shows a segmented image of a long, bent chromosome. A practical way to represent such elongated objects is by using their longitudinal axes, or medial axes, which are usually extracted with either area-based thinning or boundary-based skeletonization approaches [6,22]. In order to extract features that are invariant to chromosome bending, some determines the orientation of the minimum width enclosing rectangle [6]. On the contrary, our proposed approach for extracting the medial axis neither computes the chromosome orientation nor assumes that the chromosome is straight or only slightly bent. Furthermore, it avoids some problems that are often encountered in the skeletonization process, such as highly variable stroke directions and thicknesses of chromosomes as described in Ref. [22].

The approach for medial axis extraction proposed in this paper is based on an efficient analysis of the cross-sections of a chromosome obtained in different orientations. Most of the midpoints of such cross-sections along different orientations are very close to the medial axis. Therefore, given a sufficient number of such cross-sections, the polygonal curve computed by connecting their midpoints in the proper order will provide a good approximation to the actual medial axis. The proposed approach first obtains chromosome cross-sections along scan-lines with four equally spaced angular orientations: 0°, 45°, 90°, and 135°. Subsequently, by properly selecting the cross-sections within a specific range of their lengths, and by connecting the midpoints of the selected cross-sections in the right order, a polygonal approximation of the medial axis can be obtained.

Fig. 2 depicts the flowchart of the proposed algorithm for medial axis extraction. The algorithm consists of three stages: (a) cross-section generation and selection, (b) grouping of

Fig. 1. An image of a chromosome.

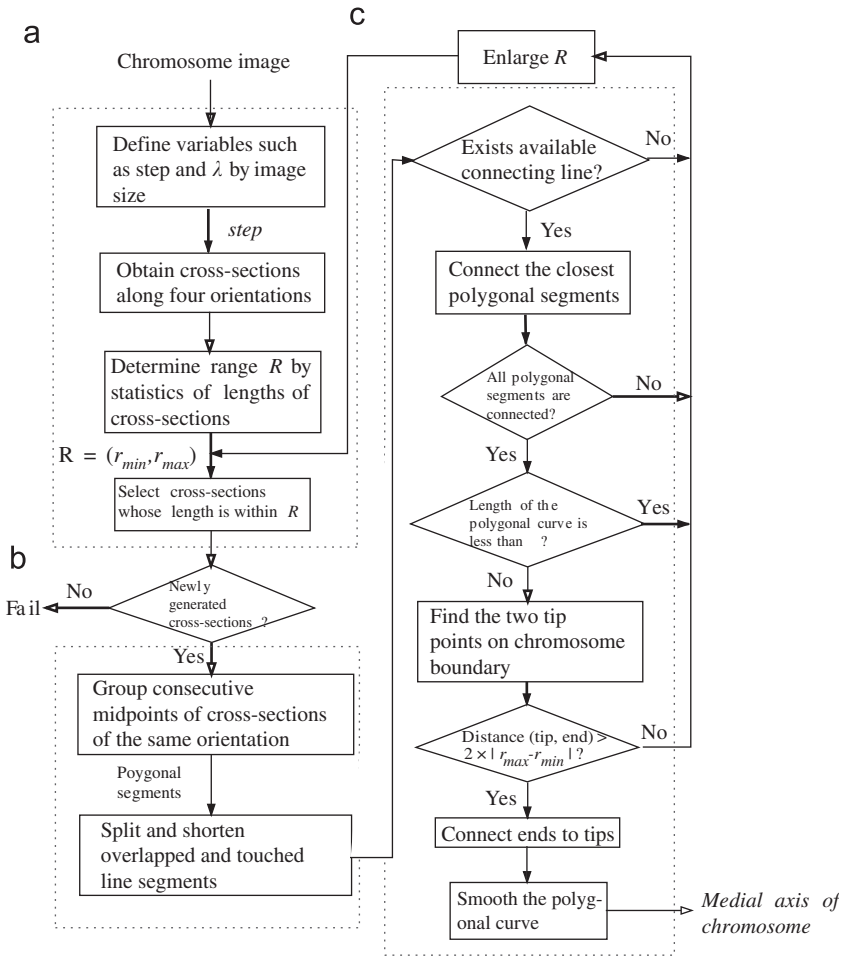

Fig. 2. The flowchart of the proposed algorithm for medial axis extraction, where (a) represents the cross-section generation and selection stage, (b) groups midpoints of cross-sections, and (c) connects polygonal segments.

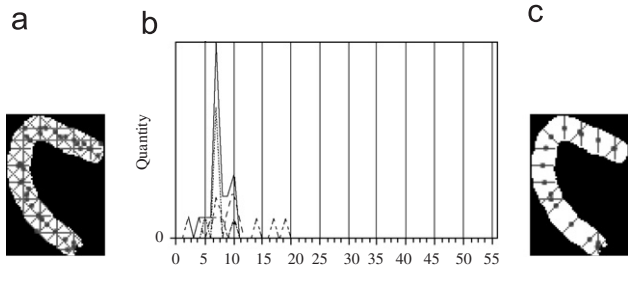

Fig. 3. (a) Cross-sections of the chromosome in Fig. 1 in four different orientations. (b) The length histogram of cross-sections in four different orientations. (c) Cross-sections whose lengths are within range R.

midpoints of cross-sections, and (c) connecting of polygonal segments, each representing a group in (b).

In stage (a), cross-sections are generated with scan-lines along the four orientations using the interval *step* determined initially as 10% of length of the longer side of the input image, as shown in Fig. 3(a). The objective of this stage is to identify and discard improper cross-sections. Since the chromosome has an elongated shape, most of the cross-sections have lengths relatively close to the width of the chromosome. To select representative cross-sections of the chromosome, we take advantage of the observation that the peaks of the four distributions are close to one another in the length histogram, e.g., ranging from 6 to 12 pixels in Fig. 3(b). A range $R = (r_{min}, r_{max})$ on the lengths is determined by this interval to select such cross-sections. Fig. 3(c) illustrates the representative cross-sections selected in this stage. Since we choose the range R to be relative to the size of the input chromosome image, it has the advantage of being adaptive to different data sets.

The medial axis of a chromosome is a simple curve and can be approximated by a series of polygonal segments. Stage (b) aims to organize the midpoints of the selected cross-sections and connect them into untouched polygonal segments. The idea is that the cross-sections obtained previously can be partitioned into several groups, each consisting of cross-sections obtained from scan-lines of the same orientation. Since the cross-sections remaining from stage (a) are the ones most likely to be perpendicular to the medial axis, the line passing through their midpoints roughly indicate the direction of the medial axis. In this stage, we group consecutive cross-sections of the same orientation, and connect the midpoints of the cross-sections within

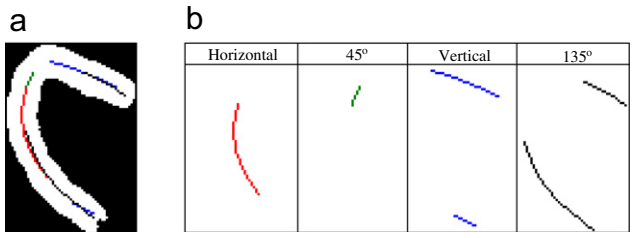

Fig. 4. (a) Polygonal segments obtained after grouping process. (b) The polygonal segments from different orientation of cross-sections are shown in the corresponding columns.

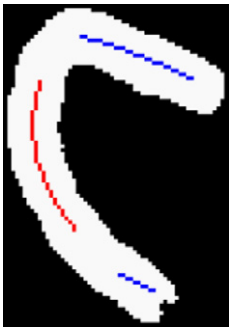

Fig. 5. The polygonal segments in Fig. 4(a) are no longer overlapped or touched to each other after the splitting and shortening process.

each group into a polygonal segment, which gives an approximation to part of the medial axis. Fig. 4(a) shows an example of such approximation, while Fig. 4(b) shows individual polygonal segments of different orientations.

Although polygonal segments are very close to the medial axis of the chromosome, it is possible that they cross or touch each other. An algorithm based on simple splitting and gradual shortening is applied to address this issue. To keep the previously obtained segments as long as possible, for each pair of polygonal segments that touch each other, the shorter one is shortened by deleting its end vertex most close to where the two segments touch. This is repeated till the two polygonal segments are separated. This process is also applied to polygonal segments that touch the boundary of the chromosome. Eventually, all of the polygonal segments are adjusted into untouched ones. Fig. 5 shows the result computed from Fig. 4(a).

The result of stage (b) is only a partial approximation of the medial axis of the chromosome. As shown in Fig. 5, there might be missing segments. This is due to either sudden bending of the chromosome or the cross-sections at that location being eliminated in stage (a). Hence, stage (c) is conducted to progressively connect the polygonal segments obtained in stage (b) into a single connected polygonal curve to derive the complete approximation of the medial axis. Specifically, we define *available connections* of the polygonal segments as those that connect end vertices of polygonal segments without crossing or touching the boundary of the chromosome. An iterative procedure is performed to connect the vertices of the shortest available connection in each iteration without generating cyclic polygonal segments. Note that if the representative cross-sections selected in stage (a) are not enough or, in other words, the range of R was too small, the polygonal segments could not be connected into a single polygonal curve successfully. If this happens, the system will enlarge R by 4 pixels, i.e., $r_{min} \leftarrow r_{min} - 2$ and $r_{max} \leftarrow r_{max} + 2$, which allows us to obtain more cross-sections, and repeat stages (a) and (b). On the other hand, we also expect that the final polygonal curve is as long as possible. An estimated chromosome length λ, which is defined as 70% of the length of the longer side of an image in stage (a), is utilized here as a lower bound. If the length of the final polygonal curve is less than λ, we also enlarge R and then repeat stages (a) and (b) in order to obtain longer polygonal segments.

Another task performed in stage (c) is to extend the polygonal curve by finding the tip points on the periphery of a chromosome image and connect them to the endpoints of the polygonal curve. Reasonable connecting lines should be perpendicular to the bands of the chromosome. Let S_i ($i = 1$ and 2) be the two endpoints of the single connected polygonal curve, and l_i ($i = 1$ and 2) be the line segment containing S_i, as illustrated in Fig. 6. A search area $\wp$ on the chromosome boundary is defined according to S_i and the direction of l_i. For any $p_j \in \wp$, if $length(\overline{p_j S_i}) > 2 \times r_{max}$, R will be enlarged and the system will repeat stages (a) and (b) again. (This happens when cross-sections around the end of the chromosome were not selected.) For each $\overline{p_j S_i}$, we obtain a chord c_j passing through the middle point of $\overline{p_j S_i}$ and perpendicular to $\overline{p_j S_i}$, as indicated in the figure, and compute the variance σ_j^2 of gray-levels along c_j. Finally, the orientation of the chord having minimum variance is assumed to be parallel to the band orientation of the chromosome, and the corresponding p_j is selected as the tip point. The polygonal curve is thus extended from S_i to p_j. Fig. 6(b) and (c) show the extended polygonal curves of two chromosomes along with their corresponding gray-level images in Fig. 6(d) and (e). The bold segments on the boundary indicate the search areas. The arrows in the figure indicate the lines connecting the endpoints to the tip points found in the search area.

The final step in stage (c) is a smoothing procedure for the extended polygonal curve. We perform linear interpolation of slopes at sample points along the extended polygonal curve. Given a point q_k^i which lies on line segment l_k, we denote the two vertices of l_k as q_k^1 and q_k^I, and the slopes of $\{l_{k-1}, l_k, l_{k+1}\}$ as $\{S_{k-1}, S_k, S_{k+1}\}$, respectively. The interpolated slope S'_{k_i} at q_k^i can be calculated by

$$S_k^i = \frac{1}{2} S_k + \frac{1}{2}\left(\frac{n}{m+n} S_{k-1} + \frac{m}{m+n} S_{k+1}\right), \quad (1)$$

where m and n denote the lengths of $\overline{q_k^1 q_k^i}$ and $\overline{q_k^i q_k^I}$, respectively. For the first line segment we let $S_0 = S_1$, and for the last line segment, $S_{K+1} = S_K$. We can then obtain a new cross-section passing through q_k^i that is perpendicular to the interpolated slope S_k^i. We apply this to every sample point on the polygonal curve, and finally obtain a new set of cross-sections. The midpoints of these new cross-sections are then connected sequentially to form the final approximation of medial axis.

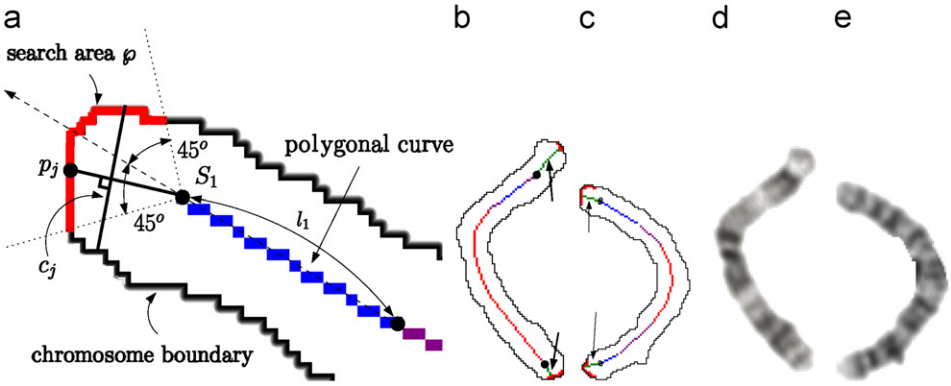

Fig. 6. (a) Extend an endpoint to a tip of chromosome. (b), (c) Two results after connecting endpoints of polygonal curves to tip points of boundaries of chromosomes. (d), (e) The corresponding gray-level images of (b) and (c), respectively.

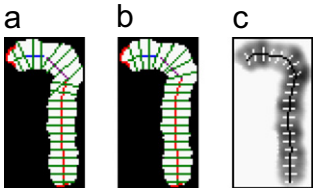

Fig. 7. An example of the smoothing process in stage (c) for a severely bent chromosome. (a) The cross-sections selected in stage (a); (b) the regenerated cross-sections using interpolated slopes; (c) the gray-level image of the chromosome overlaid with the regenerated cross-sections and the final medial axis.

Fig. 7(a) shows the cross-sections selected in stage (a) and Fig. 7(b) shows the ones newly generated using the smoothed slopes. One can see that, not only the transitions of the orientation of the cross-sections in Fig. 7(b) become more smooth than those in Fig. 7(a), but also the intersections between cross-sections are avoided. Fig. 7(c) presents the gray-level image of the chromosome overlaid with the cross-section in Fig. 7(b) and the final approximation of the medial axis.

3. Band profile extraction

The approximate medial axis is the basis for the extraction of the band profile of a chromosome. To reduce the effect of noisy data at the boundary pixels of a chromosome, and to reduce outliers caused by the bending of chromosomes and the image acquisition process, we compute the profile using a combination of gray-values sampled at $\frac{1}{4}$, $\frac{1}{2}$, and $\frac{3}{4}$ of width along each cross-section. Since the more similar two of the samples are, the more likely the other one is an outlier, we use a continuous interpolation function I'. Assume that the sorted gray-values of the three sampled pixels are denoted as I_{max}, I_{mid}, and I_{min}, respectively. We define a quadric function $f(x) = (2/D) * x^2$ where $D = I_{max} - I_{min}$, and obtain the combined gray-value using

$$I' = \begin{cases} I_c + f(I_{mid} - I_c) & \text{if } I_{mid} \geqslant I_c, \\ I_c - f(I_{mid} - I_c) & \text{if } I_{mid} < I_c, \end{cases}$$

where $I_c = (I_{max} + I_{min})/2$.

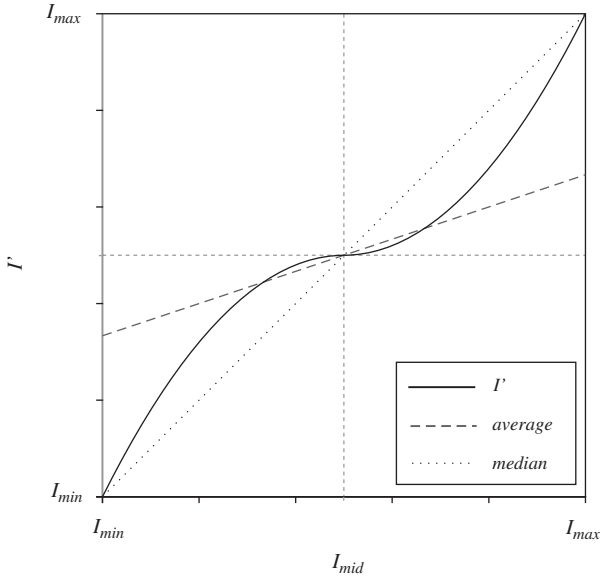

Fig. 8. The behaviors of three interpolation functions where the x-axis is the values of I_{mid} and the y-axis is the combined gray-values. The dotted curve denotes the median of the three sampled intensities. The dashed line denotes the average, and the solid curve denotes the result using our interpolation function.

Fig. 8 is a comparison of the behavior of our interpolation method and those using the median and average functions of the three sampled intensities. When the three samples are similar, our interpolation function is similar to performing their average. Otherwise, it is similar to the median function, having the effect that the most different one is treated as an outlier. For example, given 200, 200, 100 as the sampled gray-values, 100 is completely discarded and the combined result is 200.

Fig. 9(a) shows the cross-sections of the chromosome image in Fig. 1 used for band profile extraction. Each cross-section is partially shown from its $\frac{1}{4}$ to $\frac{3}{4}$ width. Fig. 9(b) presents the three curves, each representing the gray-values obtained at one of the three pixels located at $\frac{1}{4}$, $\frac{1}{2}$ and $\frac{3}{4}$ width of the cross-sections in Fig. 9(a). Fig. 9(c) shows the combined band profile

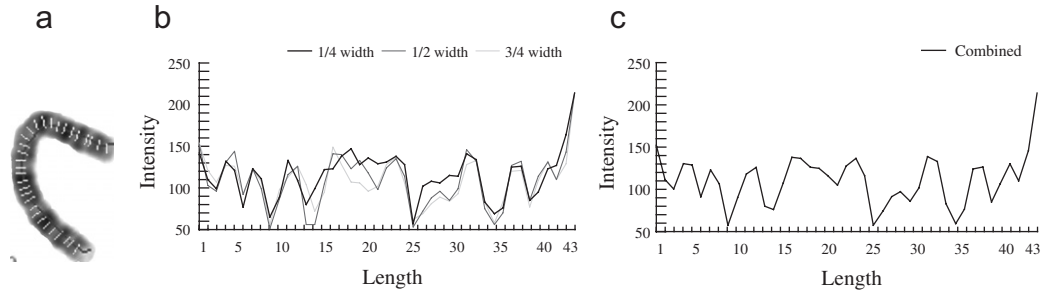

Fig. 9. (a) The cross-sections of Fig. 1 used for extract band profiles. (b) The three curves of gray-values obtained at the $\frac{1}{4}$, $\frac{1}{2}$ and $\frac{3}{4}$ width of cross-sections. (b) The final band profile obtained by combining the three curves in (b).

from the three curves in Fig. 9(b). One can see that the outliers in Fig. 9(b) are significantly reduced.

4. The classification algorithm using band profile similarity

A central task in chromosome recognition is to evaluate the similarities between known samples and the query ones. According to ISCN [5], each of the 24 categories of human chromosomes has distinct features. Common features used in the recognition or classification process include the centromere index, i.e., p/q-arm ratio, the length, and the band pattern of a chromosome. Since the chromosomes in our database do not have significant centromere features, our method of chromosome similarity evaluation is based on the band profiles obtained in Section 3, which capture the lengths and the band patterns of the chromosomes.

A band profile is a sequence of gray-values sampled along the medial axis of a chromosome and can be intuitively treated as a time sequence of a specific length. We use the term "*BP sequence*" to denote such a sampled sequence in this paper where BP stands for "band profile". Accordingly, the problem of classifying a band profile is formulated as a problem of evaluating similarity between a query BP sequence and multiple classes of BP sequences, where each class contains multiple labeled instances. Two sequences are considered similar if (i) they have enough nonoverlapping time-ordered pairs of subsequences that are similar, and (ii) their lengths are also similar. However, the sequences are usually variant on clinical practice even for homologue of the same specimen, resulting in various difficulties in evaluating the similarities. For example, BP sequences of the same class may have different lengths, making it difficult or impossible to embed the sequences in a metric space.

This paper proposes a classification approach using a novel sequence matching technique, which is an improvement over a previous method [23]. The primary focus of Ref. [23] is a data mining environment where one tries to find in a given set of sequences those are similar to a query sequence. In particular, a similarity model based on the amplitudes of subsequences is defined and the problem of determining similarity of two sequences is decomposed into three subproblems: atomic matching, window stitching, and subsequence ordering. Also, an R^+-tree is used as an indexing structure to store the transformed subsequences to achieve efficient search and to discover all similar ones in a set of sequences. In this paper, the similarity model is extended and the searching technique is improved to perform BP sequence classification. The indexing structure is also modified to store associated length information of BP sequences.

4.1. Related works on classification using band profiles

Although the standardized nomenclature [5] provides good description of features for each class of human chromosomes, the band profiles of the same class can be quite different across different batches of chromosome images in practice. In general, sources of these differences include noise in the amplitude of the profile, nonlinear size scaling along the medial axis, and intensity offset of the profile due to variations of illumination.

A number of approaches have been applied to the classification of sequences. The methods using DFT map a sequence to the frequency domain, drop all but the first few frequencies, and use them as features for classification [13,24]. An indexing structure for fast similarity search is used in Ref. [24], with the assumption that the reference data as well as query sequences are of the same length. The authors in Ref. [25] develop a more flexible approach to subsequence matching by mapping each subsequence to frequency domain. In general, Fourier analysis of the whole BP sequence has a serious drawback that the temporal information is lost. Such information often offers important nonstationary or transitory characteristics of a BP sequence.

Markov networks have been used in chromosome analysis in Refs. [16,26,27]. A band profile is quantized and represented as a chain of symbols (a string). Ref. [19] provides a comparison of performance between hidden Markov model (HMM)-based method and other approaches, including NN, singular value decomposition (SVD), principal components analysis (PCA), and fisher discriminant analysis (FDA). Although Markov models have been used with some success, quite a few parameters need to be incorporated into the model, such as transition probabilities and exclusionary and inclusionary substring probabilities to specific classes.

On the other hand, in the field of data mining and data warehousing, a number of sequence or subsequence matching ap-

proaches over time-sequence databases have been developed [23,24,28,29]. The substring matching approaches using dynamic programming and dynamic time warping techniques are also applicable, but they have some limitations when employed in practical applications [30–33]. For example, matching methods for text subsequences normally use a few discrete symbols, which result in difficulties in dealing with scaling and resolution change/variation of a sequence of real numbers. The matching process of a dynamic-time-warping-based approach also has high complexity and is computationally expensive [33].

To address the above concerns when classifying band profiles of chromosomes, we propose a novel approach wherein the similarity model and the searching technique over an indexing structure developed in Ref. [23] are improved for the classification of BP sequences. The properties that each BP sequence belongs to one of the 24 classes and that each class has a specific range of length relative to the global scale of the data set motivate the idea of grouping BP sequences by their lengths in the classification process. Moreover, a labeled BP sequence, either by an expert or by the system, can be dynamically inserted into the database as a sample of its class. Finally, previously inserted BP sequences can also be deleted on demand from the database. In the following we present more detail of our approach.

4.2. The overview of the classification system

Our approach to sequence matching for band profile classification extends the method described in Ref. [23] by incorporating the length information to improve the overall classification capability. Fixed-sized subsequences are extracted from each labeled BP sequence and then stored in a data structure together with the length information of the associated BP sequence. The database employs an R^+-tree and linked-list tables as its underlying data structure to facilitate fast search. Given the database and a query BP sequence, we classify the query sequence by examining the similarity between its subsequences and those of each chromosome class. More precisely, we first compute candidate classes for the query sequence using the length information. We then extract fixed-sized subsequences from the query BP sequence and search over the database for atomic matches between them and those of the candidate classes. Finally, the similarity for each class is obtained by evaluating the longest global match (LGM), which is a composition of the local atomic matches for that class. We outline the classification procedure for BP sequences as follows.

Building the database: We maintain a multidimensional R^+-tree that keeps fixed-sized subsequences extracted from each labeled BP sequence. The database allows multiple labeled BP sequences of the same class to be inserted, possibly from different batches of chromosome data and having different scaling and intensity offset. On the other hand, the average length of such classified BP sequences of each class is also recorded in a linked-list table. By using R^+-tree and linked-list tables, insertion and deletion of labeled BP sequences can be performed on demand without rebuilding the whole database.

Determination of candidate classes: For each class of chromosome, both the number of BP sequences labeled as that class and their average length are recorded in a linked-list table. These records are updated whenever a BP sequence is inserted or deleted. If the length of a given query BP sequence is within a predefined range around the average length of a certain class, that class is identified as a candidate class of that query sequence.

Sequence matching: Similar to the labeled BP sequences, we also extract fixed-sized subsequences from the query BP sequence before matching. For each subsequence the system finds similar ones in the R^+-tree. They may come from several labeled BP sequences, possibly from several different classes. Some constraints are then applied to stitch all local atomic matches, and a LGM is derived. The class of the query BP sequence is selected to be the same as the one that yields the LGM which satisfies the following:

(i) length of the LGM is long enough;
(ii) sum of the length of all gaps within the LGM is short enough;
(iii) length of the LGM is close to the average length of the classified BP sequences of that class.

4.3. The similarity model

Our similarity model is described in this section. Since it is an improvement over that in Ref. [23] with the utilization of length information of sequences, we start with a brief description of Ref. [23]. Fig. 10 is partially reproduced from Ref. [23] to illustrate the basic procedure of determining the similarity between two sequences. Fig. 10(a) shows two sequences S and T. Note that their lengths L_S and L_T are not the same. Instead of stretching the BP sequences to normalize them, we use multiple BP sequences of different length. In Fig. 10(b), the two sequences are first translated by their intensity offsets to align vertically. The amplitude of T is then scaled as shown in Fig. 10(c) to see whether its subsequences lie within an envelope of a pre-defined width around some corresponding subsequences of S. Fig. 10(d) shows an example where such a condition is met between subsequence pairs $\{S_1, T_1\}$ and $\{S_2, T_2\}$, respectively. These pairs are denoted as *matched subsequences*, or atomic matches, while the nonmatched subsequences, such as G_1, G_2 and G_3 in Fig. 10(e), are also identified.

With the above results, the proposed approach further classifies a query BP sequence by evaluating the similarity between the whole sequence and those being pre-classified as some instances of certain classes. The method not only searches for similar subsequences, but also investigates the satisfaction of constraints related to lengths of BP sequences. To that end, the problem is decomposed into atomic matching and window stitching, as described next.

Notations: A BP sequence is an ordered set of real values. Let $S[i]$ denote the ith element of a BP sequence S, $s[i, j]$ denote a subsequence of S from its ith element to its jth element, and $s[k]$ denote the kth element of s. We use $first(s)$ and $last(s)$ to represent the indices within S of the first and last

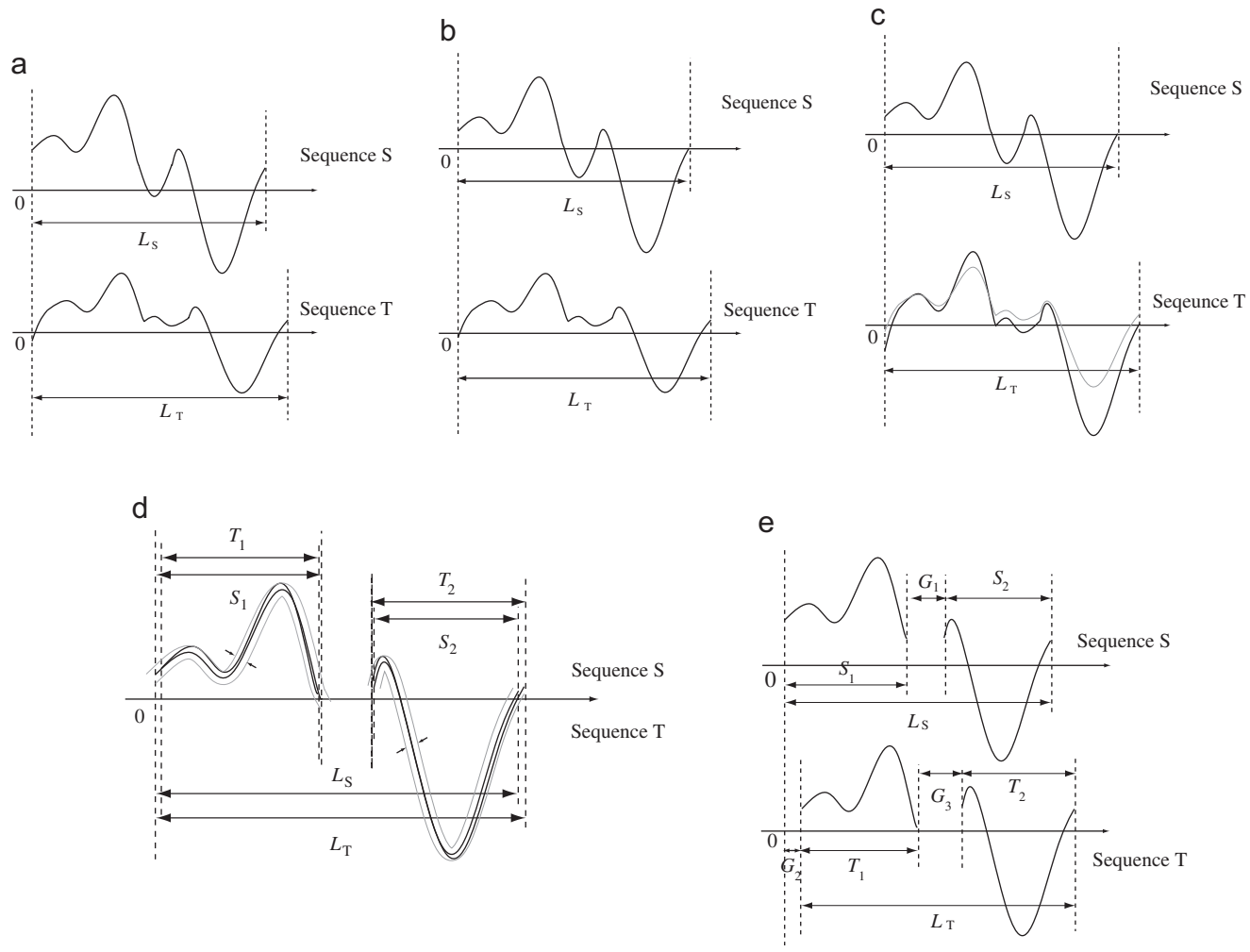

Fig. 10. Determination of similarity. (a) Two sequences. (b) Translating by their intensity offsets. (c) Amplitude scaling. (d) Subsequence matching by envelope. (e) Ignoring gaps.

elements, respectively, of a BP subsequence s. Two BP subsequences s and t overlap iff either $first(s) \leqslant first(t) \leqslant last(s)$ or $first(t) \leqslant first(s) \leqslant last(t)$. Given two BP subsequences s_p and s_q of a BP sequence S with $first(s_p) < first(s_q)$, the gap between them is defined as

$$gap(s_p, s_q) = \begin{cases} 0 & \text{if } s_p \text{ and } s_q \text{ overlap;} \\ first(s_q) & \\ \quad -last(s_p) - 1 & \text{if } s_p \text{ and } s_q \text{ do not overlap.} \end{cases}$$

Thus, given ordered BP subsequences $s_1 \ldots s_m$, the total length L_S is $last(s_m) - first(s_1) + 1$. The total gaps among BP subsequences $s_1 \ldots s_m$ is

$$gap(\{s_1, \ldots s_m\}) = \sum_{i=1}^{m-1} gap(s_i, s_{i+1}).$$

Atomic matches and window stitching: The definition of atomic matches is similar to the one defined in Ref. [23]. All the subsequences have the same length ω. The value of each element of a subsequence s is normalized according to

$$\tilde{s}[i] = \frac{s[i] - \tau_s}{\varsigma_s}. \tag{2}$$

Here $\tau_s = (s_{max} + s_{min})/2$ is the intensity offset translation, and $\varsigma_s = (s_{max} - s_{min})/2$ is the amplitude scaling, with s_{max} and s_{min} being the maximum and minimum intensity values within the subsequence s, respectively.

A subsequence of a sequence labeled as class c, $\tilde{s}_i^c$, and a subsequence of a query sequence, $\tilde{t}_j$, are regarded as similar if:

(1) The values of the ordered elements of each subsequence are similar, in the L_∞ sense as adopted in Ref. [23], i.e.,

$$|\tilde{s}_i^c[k] - \tilde{t}_j[k]| \leqslant \varepsilon \quad \text{for } 0 \leqslant k \leqslant \omega - 1. \tag{3}$$

(2) They have similar scaling:

$$\frac{1}{\kappa} \leqslant \frac{\varsigma_{\tilde{s}_i^c}}{\varsigma_{\tilde{t}_j}} \leqslant \kappa, \tag{4}$$

where $\kappa > 1$ is the scale tolerance.

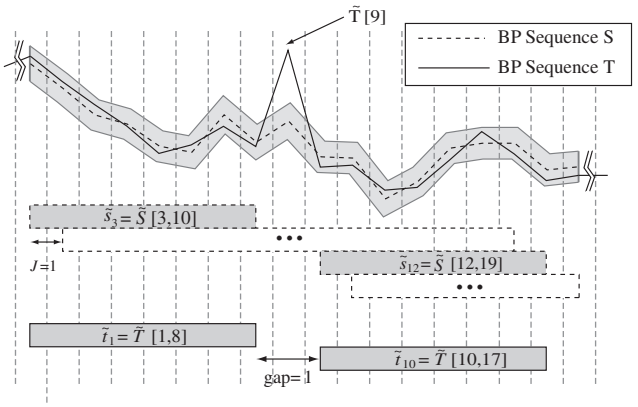

Fig. 11. Outlier and gap.

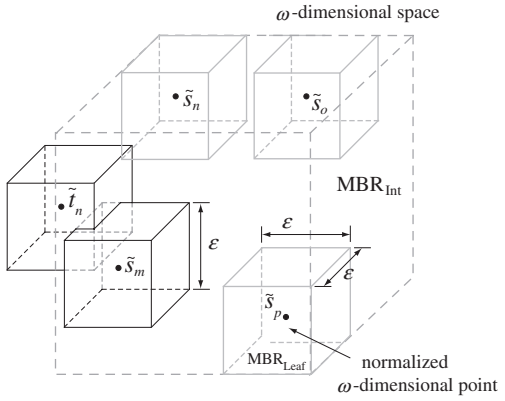

Fig. 12. An example of MBRs in ω-dimensional space for $\omega = 3$. While $\mathrm{MBR}_{\tilde{t}_n}$ is constructed by a BP subsequence of T, $\mathrm{MBR}_{\tilde{s}_m}$, $\mathrm{MBR}_{\tilde{s}_o}$, $\mathrm{MBR}_{\tilde{s}_n}$ and $\mathrm{MBR}_{\tilde{s}_p}$ are constructed by some pre-classified BP subsequences of S, respectively. In this case, these pre-classified subsequences belong to an internal node of R^+-tree, $\mathrm{MBR}_{\mathrm{Int}}$, as illustrated by the cube in dashed line. Subsequence t_n is within the envelope of subsequence s_m since their MBRs overlap.

(3) They have similar offset translation:

$$|\tau_{\tilde{s}_i^c} - \tau_{\tilde{t}_j}| \leqslant \delta, \tag{5}$$

where δ is the offset tolerance.

Fig. 11 shows an example for ω=8. $\{\tilde{s}_3 \ldots \tilde{s}_{13}\}$ and $\{\tilde{t}_1 \ldots \tilde{t}_{10}\}$ are BP subsequences of two band profiles S and T, respectively. One can see that $\tilde{T}[1] \ldots \tilde{T}$ [18] are within the envelope around $\tilde{S}$ except for $\tilde{T}$ [9]. The subsequences $\tilde{t}_2, \ldots, \tilde{t}_9$, which contain the element $\tilde{T}$ [9], are thus identified as not similar to subsequences of $\tilde{S}$ according to Eq. (3). As a result, the atomic matches between S and T are $(\tilde{s}_3, \tilde{t}_1)$and $(\tilde{s}_{12}, \tilde{t}_{10})$, with a gap of 1 element for both S and T.

For each subsequence $\tilde{t}_j$ of a query BP sequence T, the discovered atomic matches $(\tilde{s}_i^c, \tilde{t}_j)$ might come from BP subsequences of different classes of chromosome. Basically, we stitch atomic matches to derive LGM for each class based on a procedure similar to that in Ref. [23]. The LGM is obtained by applying general longest path algorithm over the underlying match graph. We present the corresponding data structure in Section 4.4 and the determination of ε, κ and δ in Section 5.

Similarity model and classifications: Unlike the similarity model proposed in Ref. [23], our model utilizes scaling and offset translation of subsequences for the local similarity measure, and length information of sequences for the global similarity measure. Let the average length of sequences labeled as class c stored in the database be L_{Avg}^c. Given a LGM consisting of M stitched atomic matches $\{(\tilde{s}_{p_1}, \tilde{t}_{q_1}), \ldots, (\tilde{s}_{p_M}, \tilde{t}_{q_M})\}$, the global similarity measure V_c for class c is defined as the sum of L_{Avg}^c and the length of the query subsequence, minus the gaps within all atomic matches and a penalty term for length difference. That is,

$$V_c = L_{Avg}^c + L_T - gap_c(\{\tilde{s}_{p_1}^c, \ldots, \tilde{s}_{p_M}^c\}) - gap_c(\{\tilde{t}_{q_1}, \ldots, \tilde{t}_{q_M}\}) - \rho \times |L_{Avg}^c - L_T|, \tag{6}$$

where ρ is the weight of length difference. A chromosome is classified as the class c^* whose corresponding LGM achieves the highest global similarity, i.e.,

$$c^* = \arg\max_c (V_c). \tag{7}$$

4.4. Data structure and algorithms

This section presents the data structure and algorithms of the proposed approach and also addresses some implementation issues. We utilize R^+-tree [34] as the indexing structure as in Ref. [23] and develop additional mechanisms to prevent node overflow during tree operations. To build the initial index structure, we scan each labeled BP sequence from end to end, extract and normalize subsequences of width ω using Eq. (2), and insert the corresponding ω-dimensional vectors into the R^+-tree. The envelope in Eq. (3) is represented by a minimum bound rectangloid (MBR) centered at the ω-dimensional point with its size being ε^ω.

Fig. 12 shows an example of MBRs in ω-dimensional space when $\omega = 3$. $\mathrm{MBR}_{\tilde{s}_m}$, $\mathrm{MBR}_{\tilde{s}_o}$, $\mathrm{MBR}_{\tilde{s}_n}$ and $\mathrm{MBR}_{\tilde{s}_p}$ are constructed by some labeled BP subsequences of S. An internal node of the R^+-tree stores a MBR enclosing all MBRs of its children, as indicated by the cube $\mathrm{MBR}_{\mathrm{Int}}$ in dashed line. $\mathrm{MBR}_{\tilde{t}_n}$ is constructed from a subsequence t_n of a query sequence T. By a query operation of R^+-tree, one can see that the subsequence t_n is within the envelope of the subsequence s_m since their MBRs overlap.

Still, several difficulties arise if we apply R^+-tree directly to store normalized BP subsequences. Since BP subsequences of one class of chromosomes may be in fact very similar to those of others, and we allow an arbitrary number of BP sequences of each class to be inserted into the database, many identical BP subsequences might be extracted. The corresponding MBRs will thus coincide in the ω-dimensional space, as indicated by $\{M, O, U\}$, $\{G, R\}$, $\{K, Q\}$, and $\{W, I\}$ in the 2D case shown in Fig. 13(a). As the branch factor of an R^+-tree node is limited, insertions of these coincident MBRs will result in many

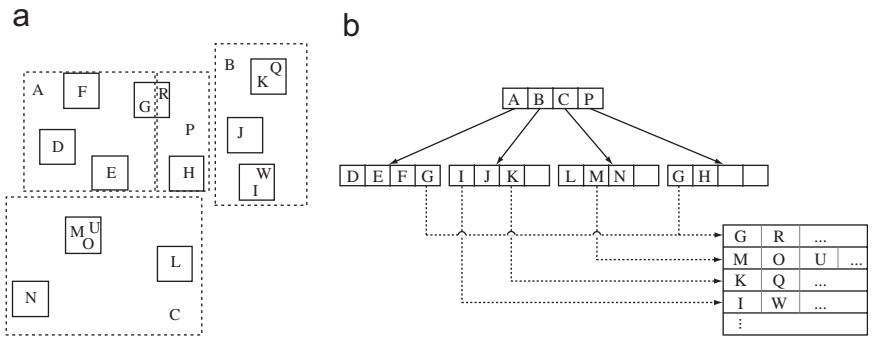

Fig. 13. (a) Some MBRs organized into an R^+-tree. (b) Cooperation of the R^+-tree structure and a track table implemented using linked-lists. The associated data of an ω-dimensional point is recorded in the *TrackTable* if the MBR was already inserted into the R^+-tree.

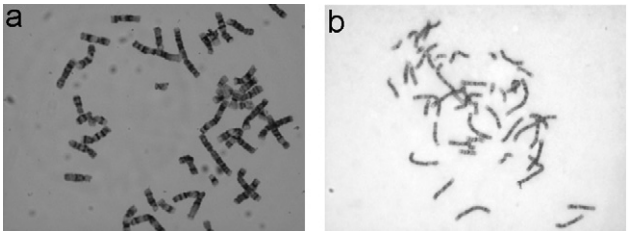

Fig. 14. Two raw images of specimens provided by (a) Cathay General Hospital, and (b) Cheng Gung Memorial Hospital, respectively.

overflowed nodes, and the induced partition operations may lead to under-filled internal and leaf nodes, making the R^+-tree grow faster than necessary and the performance being seriously reduced.

We solve this problem by introducing a linked-list table, called *TrackTable*, to track identical normalized ω-dimensional points from different chromosome classes instead of inserting the same MBRs repeatedly. Fig. 13(b) shows an R^+-tree and the associated *TrackTable*. Upon an insertion, if the MBR is identical to that of some previously inserted ones, the associated data will be recorded in *TrackTable* instead of being inserted into the R^+-tree as a new node. For example, since $\{O, U\}$ are at the same location as previously inserted $\{M\}$, they are recorded as its successors in the corresponding linked-list in *TrackTable*. For a labeled subsequence s inserted into the R^+-tree as a leaf node, the stored information includes: (1) the corresponding MBR, (2) its class-id, (3) the index of the starting element, $first(s)$, (4) its scaling factor, ς_s, and (5) its offset translation τ_s. On the other hand, the information recorded in the linked-list includes: (1) the class-id, (2) the index of the first element of the subsequence, (3) the scaling factor ς, and (4) the offset translation τ. Note that whenever a deletion of a leaf node of R^+-tree occurs, the immediate successor of the node in *TrackTable*, if any, should replace the deleted leaf node and the linked-list should also be updated for consistency.

In order to keep track of the value of L^c_{Avg} used in Eq. (6), another data structure, *LengthTable*, is also used. Let N_c be the number of labeled BP sequences of class c stored in the R^+-tree. Whenever a new BP sequence S of class c is inserted into or deleted from the data structure, the corresponding record in *LengthTable* is updated according to N_c and its length.

Algorithms: The algorithms for the proposed band profile classification system include (1) profile classification, (2) candidate class determination, (3) insertion, and (4) deletion. The main algorithm, the first one, calls the second algorithm to determine candidate classes for a query BP sequence based on the information stored in *LengthTable*, and classifies the sequence using the similarity model and the data structures

Table 1
Number of iterations required to obtain approximate medial axes of given data sets

Iterations	1	2	3	4	5	$\geqslant 6$
Percentage	49	29	12	2	1	7

Individual percentage is also listed.

Fig. 15. Three cases where the medial axes cannot be determined automatically. For each case, both gray-value and segmented binary images are shown.

Table 2
The combinations of parameter values used in the cross-validation examination

	Minimum	Maximum	Increment
ω (window size)	4	12	1
κ (scale tolerance)	1	3	0.2
δ (offset tolerance)	0	50	10
ε (envelope width)	0	0.5	0.05
ρ (weight of length difference)	0	10	2
μ (length tolerance)	0	0.5	0.1

Table 3
The average classification rate using parameters $(\omega, \kappa, \delta, \varepsilon, \rho, \mu) = (8, 2, 30, 0.2, 4, 0.2)$

Class	1	2	3	4	5	6	7	8	9	10	11	
Rate	100	100	97.1	100	88.6	82.8	91.4	77.1	94.3	91.4	97.1	
Class	12	13	14	15	16	17	18	19	20	21	22	Overall
Rate	80	88.6	88.6	85.7	85.7	94.3	88.6	91.4	94.3	91.4	74.3	90.12

Unit: %.

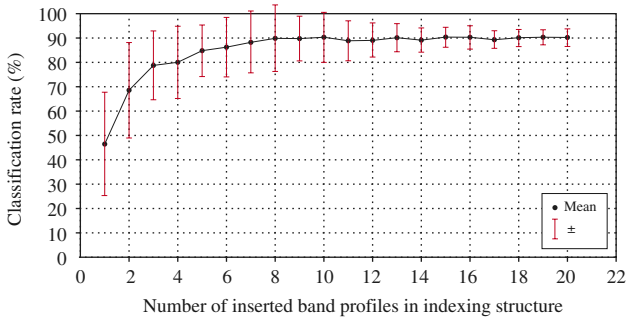

Fig. 16. Classification result over the database provided by Cheng Gung Memorial Hospital using the parameters determined in phase 1.

described above. When a labeled BP sequence is inserted into the R^+-tree with the third algorithm, it is the extracted BP subsequences that are actually stored, while the BP sequence itself is directly copied to a repository database. An inserted sequence can be reviewed or deleted on demand form the database with the fourth algorithm.

5. Experimental results

The data sets of chromosome images used in the experiments are provided by Cathay General Hospital (13 specimens) and Cheng Gung Memorial Hospital (78 specimens). Fig. 14 shows two raw images of the two data sets, respectively. Different scaling and offset translation, truncation, noise due to debris, overlapping and touching among chromosomes, etc., are present in these data sets. The segmentation of the raw images into images of individual chromosomes, including the labeling of chromosome and background pixels, is carried out by Lumens Digital Optics, Inc. The largest image size is 40×132 pixels. In the following, the experimental results are presented separately for medial axis extraction and the classification of BP sequences.

Medial axis extraction: The proposed approach for medial axis extraction is applied to all segmented chromosomes in the data sets. Since the proposed method of band profile extraction is insensitive to the exact location of the medial axis, the goal is *not* to extract an ideal but rather a simple polygonal approximation of the medial axis. Table 1 gives a summary of the required number of iterations for the algorithm in Fig. 2 over the given data sets. For the total of 4186 chromosomes from the two data sets, the algorithm is able to automatically extract 99.7% (4170) of them, with most of them (78%) computed within two iterations.

Upon further inspection, the required number of iterations is mainly related to the shape of a chromosome, and is independent of its class association. Chromosomes which are severely bent or have irregular shapes usually require more iterations to find the medial axes. Unsuccessful cases (16 out of 4186) are mainlydue to poor segmentation of overlapping and touching chromosome images. Fig. 15 gives three examples where the medial axes cannot be determined automatically. One can see that the boundaries of these segmented chromosome images are extremely irregular, so that stage (c) in Fig. 2 fails to connect polygonal segments into a single polygonal curve.

Classification of BP subsequences: The experiment for classification consists of two phases: the determination of the optimal parameter set and the performance evaluation of the system using that parameter set. In the first phase, since the numbers of *X*-class and *Y*-class chromosomes of the disjoint subsets vary significantly, we skip these two classes of chromosomes. We perform 5-fold cross-validation examination on the data set of Cathay General Hospital over six system parameters (ω, κ, δ, ε, ρ and μ). The combinations of these parameters used in this examination are listed in Table 2.

For each combination of the parameters, e.g., $(\omega, \kappa, \delta, \varepsilon, \rho, \mu) = (5, 1.4, 10, 0.5, 6, 0.2)$, a cross-validation trial is performed as follows. The data set is partitioned into five subsets. Of the five subsets, a single subset is retained as test (query) data, and the remaining four subsets are used as training data for building the database using that combination of parameters. The process is repeated five times, with each of the five subsets used exactly once as the test data. The five resulting classification rates are then averaged to produce an overall classification rate. The combination of parameters that produces the highest average classification rate is selected as the optimal parameter set.

The average time to build the database of 242 BP sequences for one trial is 12.3 s on a notebook equipped with a 1.7 GHz Pentium IV processor and 512 MB of system memory, and the final height of the R^+-tree is 6. The average time of classification spent for one trial is 3.3 s, hence the system approximately spends 0.075 s to classify a BP sequence. Table 3 shows the average classification rate using the combination of parameters $(\omega, \kappa, \delta, \varepsilon, \rho, \mu) = (8, 2, 30, 0.2, 4, 0.2)$, which gives the highest average classification rate (90.1%).

The purpose of phase 2 is to evaluate the average classification rate with respect to different databases built with different numbers of chromosomes using the optimal parameter set. We perform phase 2 on the data set provided by Cheng Gung Memorial Hospital. Twenty runs are carried out and each run

is executed 20 times. In each execution of the *i*th run, *i* labeled BP sequences of each class are randomly drawn from the data set and inserted into the database. The remaining BP sequences are then used as test data. We plot in Fig. 16 the correct classification rate versus *i*. One can see that the average classification rate approaches 90% when the number of inserted band profiles for each class approaches 8. Moreover, the standard deviation narrows to below 5% after the number of inserted band profiles exceeds 15.

6. Conclusion

Automated chromosome classification is an essential task in cytogenetics. Numerous attempts have been made to characterize chromosomes to perform clinical and cancer cytogenetics research. In this paper we propose novel approaches for medial axis extraction and band profile classification without using the centromere feature. In particular, the medial axis is obtained by simple cross-section analysis and the classification is based on local subsequence similarity match and global length information. Two data sets are used for the determination of system parameters and the evaluation of system performance, respectively. One desirable feature of the proposed approach is the possibility of dynamic insertion and deletion of BP sequences without rebuilding the database, which enhances the usability and flexibility of the classification system. According to the experimental results, the developed classification system can efficiently compute band profiles of the chromosomes along the extracted medial axes, and obtain satisfactory classification results.

References

[1] B. Lerner, Toward a completely automatic neural-network-based human chromosome analysis, IEEE Trans. Systems Man Cybern. 28 (1998) 544–552.

[2] X. Wang, B. Zheng, M. Wood, S. Li, W. Chen, H. Liu, Development and evaluation of automated systems for detection and classification of banded chromosomes: current status and future perspectives, J. Phys. D: Appl. Phys. 38 (2005) 2536–2542.

[3] C.U. Garcia, A.B. Rubio, F.A. Perez, F.S. Hernandez, A curvature-based multiresolution automatic karyotyping system, Mach. Vision Appl. 14 (2003) 145–156.

[4] L.V. Guimaraes, A. Schuck, A. Elbern, Chromosome classification for karyotype composing applying shape representation on wavelet packet transform, in: Proceedings of the 25th Annual International Conference on IEEE EMBS, Cancun, Mexico, 2003, pp. 941–943.

[5] ISCN1985: An international system for human cytogenetics nomenclature, in: D.G. Harnden, H.P. Klinger (Eds.), Cytogenetics and Cell Genetics, Karger, Basel, 1985.

[6] J. Piper, E. Granum, On fully automatic feature measurements for banded chromosome classification, Cytometry 10 (1989) 242–255.

[7] G.C. Charters, E. Granum, Trainable grey-level models for disentangling overlapping chromosomes, Pattern Recognition 32 (1999) 1335–1349.

[8] A. Carothers, J. Piper, Computer-aided classification of human chromosomes: a review, Stat. Comput. 4 (1994) 161–171.

[9] B. Lerner, H. Guterman, I. Dinstein, Y. Romem, Medial axis transform based features and a neural network for human chromosome classification, Pattern Recognition 28 (1995) 1673–1683.

[10] G. Ritter, G. Schreib, Using dominant points and variants for profile extraction from chromosomes, Pattern Recognition 34 (2001) 923–938.

[11] C.A. Groen, K. Kate, A.W.M. Smeulders, T. Young, Human chromosome classification based on local band descriptors, Pattern Recognition Lett. 9 (1989) 211–222.

[12] G. Ritter, G. Schreib, Profile and feature extraction from chromosomes, in: Proceedings of the 15th International Conference on Pattern Recognition, vol. 2, Barcelona, Spain, 2000, pp. 287–290.

[13] A. Moller, H. Nilsson, T. Caspersson, G. Lomakka, Identification of human chromosome regions by aid of computerized pattern analysis, Exp. Cell Res. 70 (1972) 475–478.

[14] E. Granum, T. Gerdes, C. Lundsteen, Simple weighted density distributions, WDD's for discrimination between G-banded chromosomes, in: Proceedings of the Fourth European Chromosome Analysis Workshop, Edinburgh, Scotland, 1981.

[15] C. Lundsteen, T. Gerdes, J. Maahr, Automatic classification of chromosomes as part of a routine system for clinical analysis, Cytometry 7 (1985) 1–7.

[16] J. Gregor, E. Granum, Finding chromosome centromeres using band pattern information, Comput. Biol. Med. 21 (1991) 55–67.

[17] W.P. Sweeney, M.T. Musavi, J.N. Guigi, Classification of chromosomes using a probabilistic neural network, Cytometry 16 (1994) 17–24.

[18] P.A. Errington, J. Graham, Application of artificial neural networks to chromosome classification, Cytometry 14 (1993) 627–639.

[19] J.M. Conroy, T.G. Kolda, D.P. O'Leary, T.J. O'Leary, Chromosome identification using hidden markov models: comparison with neural networks, singular value decomposition, principal components analysis, and Fisher discriminant analysis, Lab. Invest. 80 (2000) 1629–1641.

[20] P. Biyani, X. Wu, A. Sinha, Joint classification and pairing of human chromosomes, IEEE/ACM Trans. Comput. Biol. Bioinformatics 2 (2005) 102–109.

[21] W.C. Schwartzkopf, A.C. Bovik, B.L. Evans, Maximum-likelihood techniques for joint segmentation–classification of multispectral chromosome images, IEEE Trans. Med. Imaging 24 (2005) 1593–1610.

[22] L. Lam, S.-W. Lee, C.Y. Suen, Thinning methodologies—a comprehensive survey, IEEE Trans. Pattern Anal. Mach. Intell. 14 (1992) 869–885.

[23] R. Agrawal, K.I. Lin, H.S. Sawhney, K. Shim, Fast similarity search in the presence of noise, scaling, and translation in time-series databases, in: Proceedings of the 21st International Conference on Very Large Databases, Morgan Kaufmann, Zurich, Switzerland, 1995, pp. 490–501.

[24] R. Agrawal, C. Faloutsos, A.N. Swami, Efficient similarity search in sequence databases, in: D. Lomet (Ed.), Proceedings of the Fourth International Conference on Foundations of Data Organization and Algorithms, Springer, Chicago, IL, 1993, pp. 69–84.

[25] C. Faloutsos, M. Ranganathan, Y. Manolopoulos, Fast subsequence matching in time-series databases, in: Proceedings of the 1994 ACM SIGMOD International Conference on Management of Data, Minneapolis, MN, 1994, pp. 419–429.

[26] E. Granum, M.G. Thomason, J. Gregor, On the use of automatically inferred Markov networks for chromosome analysis, in: Automation of Cytogenetics, Springer, Berlin, 1989, pp. 233–251.

[27] E. Granum, M.G. Thomason, Automatically inferred Markov network models for classification of chromosomal band pattern structures, Cytometry 11 (1990) 26–39.

[28] D. Rafiei, A. Mendelzon, Similarity-based queries for time series data, in: Proceedings of the 1997 ACM SIGMOD International Conference on Management of Data, Tucson, Arizona, 1997, pp. 13–25.

[29] Y.S. Moon, K.Y. Whang, W.S. Han, General match: a subsequence matching method in time-series databases based on generalized windows, in: Proceedings of the 2002 ACM SIGMOD International Conference on Management of Data, Madison, Wisconsin, 2002, pp. 382–393.

[30] M. Roytberg, A search for common patterns in many sequences, Comput. Appl. Biosci. 8 (1992) 57–64.

[31] J.T.L. Wang, G.W. Chirn, T.G. Marr, B. Shapiro, D. Shasha, K. Zhang, Combinatorial pattern discovery for scientific data: some preliminary results, in: Proceedings of the 1994 ACM SIGMOD International Conference on Management of Data, Minneapolis, MN, 1994, pp. 115–125.

[32] B.W. Erickson, P.H. Sellers, Recognition of patterns in genetic sequences, in: D. Sankoff, J.B. Kruskal (Eds.), Time Warps, String Edits, and

Macromolecules: The Theory and Practice of Sequence Comparison, Addison-Wesley, Reading, MA, 1983, pp. 55–90.

[33] D. Berndt, J. Clifford, Using dynamic time warping to find patterns in time series, in: KDD94: AAAI Workshop on Knowledge Discovery in Databases, Seatle, WA, 1994, pp. 359–370.

[34] T.K. Sellis, N. Roussopoulos, C. Faloutsos, The R^+-tree: a dynamic index for multi-dimensional objects, in: Proceedings of the 12th International Conference on Very Large Databases, Brighton, England, 1987, pp. 507 –518.

About the Author—JEN-HUI CHUANG is a professor at the Department of Computer Science at National Chiao Tung University. He received the B.S. degree in Electrical Engineering from National Taiwan University in 1980, the M.S. degree in Electrical and Computer Engineering from the University of California at Santa Barbara in 1983, and the Ph.D. degree in Electrical and Computer Engineering from the University of Illinois at Urbana-Champaign in 1991. Since 1991, he has been on the faculty of the Department of Computer Science at National Chiao Tung University. His research interests include robotics, computer vision, 3-D modeling, speech and image processing, and VLSI systems. Dr. Chuang is a senior member of IEEE and the Tau Beta Pi Society.

About the Author—TSAIPEI WANG is an assistant professor of the Department of Computer Science at National Chiao Tung University. He received the Ph.D. degree in Physics from University of Oregon in 1999. He received the M.S. degree in Computer Science from University of Missouri-Columbia in 2002, and the Ph.D. degree in Computer Engineering and Computer Science from University of Missouri-Columbia in 2005. From 2002 to 2005, he was a Postdoctoral Fellow in the Department of Electrical and Computer Engineering, University of Missouri-Columbia. His research interests include image Processing, pattern recognition, fuzzy Systems, computer vision and computer graphics.

Abour the Author—JAU-HONG KAO is now a Ph.D. student at the Computer Science Department at National Chiao Tung University. He received the B.S. degree in Surveying from National Cheng Kung University in 1997, and the M.S. degree in Computer and Information Science from National Chiao Tung University in 1999. His research interests include image Processing, pattern recognition,computer vision and computer graphics.